Computer simulation of intrinsic defects in $PbWO_4$

Qisheng Lin, Xiqi Feng,* and Zhenyong Man
Laboratory of Functional Inorganic Materials, Chinese Academy of Sciences, 1295 Dingxi Road, Shanghai 200050, People's Republic of China

(Received 19 September 2000; published 6 March 2001)

A computer simulation study has been performed to investigate the intrinsic defects in $PbWO_4$ (PWO). The interatomic potentials were empirically fit to the known crystal properties. Calculations reveal that PbO nonstoichiometry dominates the intrinsic defects in PWO, whereas the oxygen Frenkel defects will only be significant at high temperature. Through binding-energy calculations, defect clusters are predicated to actually exist in the material. An analysis of activation energy corroborates that oxygen vacancy migration is the mobile ionic defect in PWO, moreover, isotropic conduction is suggested despite the tetragonal symmetry of the crystal. The concentration dependence of electronic defects on the oxygen partial pressure is also studied.

DOI: 10.1103/PhysRevB.63.134105 PACS number(s): 61.72.Bb, 61.72.Hh, 61.72.Ji, 61.82.Ms

I. INTRODUCTION

High-oxide ion conducting solids with fluorite-type structure have been found to have potential use for electrolyte materials of the solid oxide fuel cell and oxygen gas sensor.[1] Lead tungstate, $PbWO_4$(PWO), is also expected to be a good oxide ion conductor because of its tetragonal scheelite-type structure, which can be derived from the fluorite-type structure. As a matter of fact, the rare-earth ions substituted for PWO have been found to represent oxide ion conductivity.[2,3]

More recently, the PWO crystal has attracted increasing attention because of its application as a new generation of scintillator in high-energy physics.[4–6] Until now so much progress has been made that the compact muon solenoid electromagnetic calorimeter has reached its final research and development phase.[7–15] However, there are still issues in debate,[9,13–15] e.g., the origin of the color center absorption bands in the short wavelength region. Generally, color center absorption bands, which are the ''footprint'' of defects, are harmful to scintillators. They will degrade the crystal radiation hardness and lower the light output. How to eliminate this kind of negative effect, therefore, becomes one of the most important works in PWO crystal.

Due to the limited knowledge about the defects in PWO, we still cannot come to an agreement on the nature of those color centers despite that we have studied the intrinsic and extrinsic defects with powerful tools, e.g., electron spin resonance.[13–15] However, the resolution of this problem is rather important for ameliorating the scintillation properties, understanding the radiation damage mechanism, and offering some directions for batch crystal growth.

We tried to study the intrinsic and extrinsic defects in PWO crystals with the computer simulation techniques that have never been used in this system, so that an overview of the defects can be achieved. In this paper, the intrinsic-defect-based properties are discussed, leaving the results of the extrinsic defects to be reported in another paper. The context of this paper is comprised of the results and discussions on intrinsic defects, cluster stability, oxygen migration, and redox reaction, in turn presented in Sec. III, after we have outlined in Sec. II the simulation methods. The conclusions are summarized in Sec. IV.

II. SIMULATION METHODS

The lattice simulations were performed using the General Utility Lattice Program (GULP) program that is based upon the Mott-Littleton methodology[16] for accurate modeling of perfect and defect lattices. Since detailed documentation of the simulation techniques can be found elsewhere,[17,18] only a brief account will be presented here.

An important feature of these calculations is the modeling of defects. The simplification of the Mott-Littleton method is to divide the crystal lattice that surrounds the defect into three regions known as 1, 2a, and 2b.[16,19,20] In the inner region, all interactions are treated at an atomistic level and the ions are explicitly allowed to relax in response to the defect, while the remainder of the crystal, where the defect forces are relatively weak, is treated by more approximate quasicontinuum methods. In this way, local relaxation is effectively modeled and the crystal is not considered simply as a rigid lattice through which ion species diffuse. In this study, the inner defect region was set 7.5 Å, which was found to be adequate for the convergence of the computed energies.

Both perfect- and defect-lattice calculations are formulated within the framework of the Born-like model.[21] In this approximation, the potentials describing the interatomic interactions between two ions, with distance r, are presented as follows,

$$U_{ij}(r)=\frac{Z_iZ_je^2}{r}+A_{ij}\exp\left(\frac{-r}{\rho_{ij}}\right)-\frac{C_{ij}}{r^6}, \qquad (2.1)$$

where the first part is the long-range Coulombic term and the latter are the short-range term described by the two-body Buckingham form. Therefore, Z_i is the formal charge of atom i, and A_{ij}, r_{ij}, and C_{ij} are the adjustable potential parameters.

Because charged defects will polarize other ions in the lattice, ionic polarizability (a) is also incorporated into the potential model. A shell-model[22] treatment of such effects is described in terms of a shell with charge Y connected via an isotropic harmonic spring of force constant k to a massive core of charge Z-Y, namely,

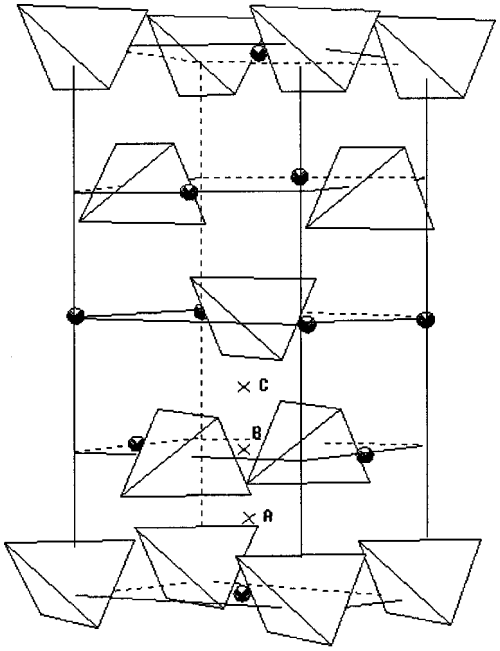

FIG. 1. Unit cell of $PbWO_4$ crystal structure. (×) denotes the possible interstitial sites.

$$a = \frac{Y^2}{k}. \tag{2.2}$$

We note that in the context of the Coulombic term, an integral ionic charge were presumed, i.e., 2+ for Pb, 6+ for W, 2− for O, so that a straightforward definition of hole states such as Pb^{3+} or O^- can be achieved.

A crucial test of any theoretical study of solid-state materials is the accurate simulation of the crystal structure. In our investigation, the crystal structure of Moreau,[23] shown in Fig. 1, was simulated. The oxygen-oxygen and tungsten-oxygen short-range interaction parameters were transferred directly from recent simulation of Bi_2WO_6,[24] and the lead-oxygen and lead-lead potential parameters were transferred from perovskite $PbTiO_3$.[25] Using these potential parameters, lattice parameters with errors of about 2% can be reproduced. Due to the changes in the cation coordination number between PWO and $PbTiO_3$ however, we recognize that a ''correction factor'' [26] should be added. The Pb-related (i.e., the Pb-Pb and Pb-O) short-range potential parameters, therefore, were treated as variables in a ''relax fitting'' procedure.[17] The final resulted potentials and shell-model parameters, which are used in the following simulation of defects, are given in Table I.

The comparison between the calculated lattice parameters and bond distances using potential parameters we have derived, and the experimentally determined values are tabulated in Table II. The lattice parameters vary by an average of 0.15% from the experimental values. Such a good agreement between the simulated and the experimental structure indicates the validity of our model, even though, unfortunately, no additional experimental data for further validation and refinement of the potential model are available. The interatomic potential model for PWO, therefore, provides a good basis for the defect calculations.

TABLE I. Empirically derived potential parameters used in $PbWO_4$. The maximum short-range potential cutoff is 12.0 Å.

(a) Short-range potential parameters

Interactions	A (eV)	ρ (Å)	C (eV Å^6)
Pb^{2+}-Pb^{2+}	18 912.1140	0.313 781	2.600 0
Pb^{2+}-O^{2-}	8 086.803 8	0.264 866	3.563 6
W^{6+}-O^{2-}	767.430 0	0.438 600	0.000 0
O^{2-}-O^{2-}	9 547.960 0	0.219 200	32.000

(b) Shell parameters

Species	Y (e)	k (eV Å^{-2})
Pb^{2+}	−0.09	21 006.539
W^{6+}	5.89	7.690
O^{2-}	−2.04	6.300

III. RESULTS AND DISCUSSION

A. Intrinsic disorder

Energy calculations of intrinsic defects were performed on the isolated point defects (namely the vacancy and interstitial defects). These defect energies are given in Table III. Figure 1 shows the possible interstitial sites we have considered. These sites are considered according to the general chemistry and crystal structure knowledge. It was found that interstitial oxygen ions were most favorable on the *C* site, while the interstitial lead ions were preferentially on the *B* site. Note that we have also placed the *W* interstitial at several possible locations in the structure, but on every case, the energy minimization tended to divergence, indicating that it is impossible to create *W* interstitial or *W* Frenkel defects according to this model.

Five types of intrinsic disorder (Frenkel and Schottky disorders) that may influence the defect properties of PWO are given as follows,

$$Pb_{Pb}^{\times} = V''_{Pb} + Pb_i^{\cdot\cdot}, \tag{3.1}$$

$$O_O^{\times} = V_O^{\cdot\cdot} + O_i'', \tag{3.2}$$

TABLE II. Calculated properties of perfect crystal of $PbWO_4$.

Properties	Calculated	Experimental (Ref. 23)
Lattice energy (eV/formula)	−247.67	
Unit cell parameters (Å)		
a	5.441	5.456
c	12.024	12.020
Bond distances (Å)		
Pb-O	2.574	2.58
	2.733	2.64
W-O	1.731	1.79

TABLE III. Calculated energies of atomic defects in $PbWO_4$.

(a) Isolated point defects			
Defect	Energy (eV)	Defect	Energy (eV)
V''_{Pb}	25.55	$Pb_i^{\cdot\cdot}$	−13.19
$V_O^{\cdot\cdot}$	18.72	O_i''	−9.46
$V_W^{6\prime}$	178.67	W_i^{6+}	
(b) Frenkel and Schottky disorder			
Frenkel-type	Energy (eV/defect)	Schottky-type	Energy (eV/defect)
Oxygen	4.63	PbO	2.74
Lead	6.13	WO_3	5.36
		$PbWO_4$	5.24

$$\text{`PWO'} = V''_{Pb} + V_O^{\cdot\cdot} + \text{PbO}, \tag{3.3}$$

$$\text{`PWO'} = V_W^{6\prime} + 3V_O^{\cdot\cdot} + WO_3, \tag{3.4}$$

$$\text{`PWO'} = V''_{Pb} + V_O^{\cdot\cdot} + V_W^{6\prime} + PbWO_4. \tag{3.5}$$

In order to calculate the energies of Schottky disorder, lattice energies ($E_{PbO} = -37.89$ eV and $E_{WO_3} = -213.38$ eV) which are calculated consistently using the potential parameters given in Table I, must be incorporated. The calculated formation energies per defect are also presented in Table III.

Examination of the formation energies clearly reveals that the predominant disorder manner is of the PbO nonstiochoimetry [Eq. (3.3)], whereas the oxygen Frenkel defect will only be significant at higher temperature. These results agree well with observations and the conductivity measurements.[27–29] Since the energies of Pb Frenkel and WO_3 non-stoichiometry are much higher, their contribution to intrinsic defect formation is negligible. However, high concentrations of intrinsic defects are not expected in light of the calculated reaction energies, even if one takes into account the vacancy clusters, a point to which we will return below. In fact, the experimental PbO deviation was about 1000 ppm.[30]

B. Clustering stability

In this section, we will investigate the stability of the $(V''_{Pb}:V_O^{\cdot\cdot})$ pair and $(2V''_{Pb}:V_O^{\cdot\cdot})$ clusters. The simulation approach is carried out via calculating the cluster binding energies with respect to the constituent defects. The binding energy is defined as the difference between the sum of the formation enthalpies of the constituent point defects and the formation enthalpy of the appropriate defect cluster:

$$E_b = E_{\text{cluster}} - [\Sigma E_{\text{defects}}]. \tag{3.6}$$

Since the interaction in clusters is primarily electrostatic, oppositely charged defects in nature attempt to minimize their separation. However, the displacement of ions surrounding a defect, i.e., the lattice relaxation, must also be considered because it may conflict with electrostatic effects. The cluster geometry, therefore, is of most importance when considering its stability. Table IV presents the calculated binding energies of the simple pair with first (*nn*), second (*nnn*) and third neighbor (*nnnn*) sites as well as the $(2V''_{Pb}:V_O^{\cdot\cdot})$ cluster with [1st: 2nd] separation (there is not the [1st:1st] configuration in this crystal). To assist in the comparison of clusters with different configuration, the binding energies are given per constituent defect in the cluster.

TABLE IV. Calculated binding energies for clusters in $PbWO_4$.

Configuration	Separation (Å)	Binding energies (eV/defect)
$(V''_{Pb}:V_O^{\cdot\cdot})$	*nn* (2.574)	−1.37
$(V''_{Pb}:V_O^{\cdot\cdot})$	*nnn* (2.733)	−1.41
$(V''_{Pb}:V_O^{\cdot\cdot})$	*nnnn* (4.007)	−1.46
$(2V''_{Pb}:V_O^{\cdot\cdot})$	[1st:2nd]	−0.56

The results reveal two main points. First, the binding energies, hence the stability of a simple pair of the *nnnn* configuration is greater than other configurations, indicating strong lattice relaxation of *in situ* situation. Obviously, the negative binding energies are helpful to decrease the reaction energy of Eq. (3.3), making the PbO disorder easier to occur. Second, both the simple pairs and cluster are found bound with negative binding energies. This would suggest that, besides the neutral $(V''_{Pb}:V_O^{\cdot\cdot})$ simple pair, the negative charged clusters, $(2V''_{Pb}:V_O^{\cdot\cdot})$, are predicated existing in PWO crystals. Note we have also investigated the stability of clusters in which a lead vacancy is associated with two oxygen vacancies. In every case, it tends to divergence, suggesting the cluster is unstable. These results, in general, corroborate our results based on extended x-ray-absorption fine structure, x-ray diffraction and optical experiments.[31]

We recall that the conclusions mentioned above do not exclude the possibility that more complex clusters might exist in PWO. This, however, is clearly beyond our calculations since we have here considered only the contents within a unit cell.

C. Oxygen vacancy migration

It has been well established that oxygen vacancy is the mobile ionic defect in PWO crystals.[28,29] However, the knowledge, with respect to the nature of a migration mechanism or pathway, is still vacant. Simulation methods can enhance our understanding of this problem by evaluating the activation energy of mobile ion.

For PWO, we estimated the activation energies by calculating the defect energies along the migration path between adjacent oxygen sites of WO_4 tetrahedron. In this way, the saddle-point configuration can be identified from which the energy barrier to migration is derived. We recognize there are six possible pathways, as shown in Fig 2, for oxygen vacancy migration. The derived activation energies are reported in Table VI.

An examination of the results shows that the oxygen ion migration through *V*1 and *V*2 pathways has a high barrier (>1.9 eV), suggesting such migration has little contribution to conductivity. However, we can easily discern a low-energy pathway involves a zigzag-type mechanism between

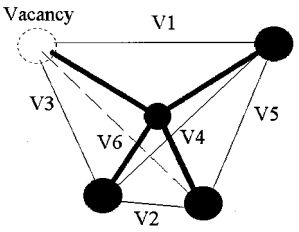

FIG. 2. Schematic of the possible migration paths for oxygen vacancies along the WO_4 tetrahedron edge.

adjacent apical oxygen atoms, e.g., $V3 \rightarrow V4 \rightarrow V5 \rightarrow V6$. The calculated activation energy of 0.48 eV accords well with the experimental value (0.40 eV) obtained from the ionic conductivity measurement at temperatures lower than 780 °C,[29] in which region defect association is believed to be less significant. This type of migration pathway suggests an isotropic conduction of PWO, despite the tetragonal symmetry. We note this phenomenon is not a new one.[28] As a matter of fact, besides PWO, the isostructural $CaWO_4$ crystal also appears as an isotropic conduction.[32] From this viewpoint, the explanation of the quasi-fourfold symmetry in the scheelite $CaWO_4$ crystal[33] is also valid for PWO.

D. Redox reaction

It is important to consider the reaction of defects in response to the variation of oxygen partial pressure because the PWO, as scintillation crystals, are always annealed in air or oxygen atmosphere.[7] We have considered the following two possible oxidation reactions [Eqs. (3.7) and (3.8)] and one reduction reaction [Eq. (3.9)]:

$$\text{`PWO'} + V_{\text{O}}^{\cdot\cdot} + \tfrac{1}{2}\text{O}_2 \rightarrow \text{O}_{\text{O}}^{\times} + 2h^{\cdot} \tag{3.7}$$

$$\text{`PWO'} + \tfrac{1}{2}\text{O}_2 \rightarrow O_i'' + 2h^{\cdot} \tag{3.8}$$

$$\text{`PWO'} \rightarrow V_{\text{O}}^{\cdot\cdot} + 2e' + \tfrac{1}{2}\text{O}_2 . \tag{3.9}$$

In order to calculate the reaction energy of these equations, one should acquire the defect energy of electronic defects (namely the hole and electron) first. According to the linearized-augmented-plane-wave calculations,[34] the valence bands of PWO consist of mainly the O $2p$ states and the conduction bands of W $5d$ states. And the Pb $6s$ states form a narrow band 1 eV below the bottom of the valence bands and also hybridize with states throughout the valence bands, while the Pb $6p$ states hybridize with states throughout the conduction bands. To simplify the treatments, our approach regarding electronic defects follows from the method that has been successfully modeled in La_2CuO_4,[35,36] $KTaO_3$,[37] $Ba_2In_2O_5$,[38] $HgBa_2Ca_2Cu_3O_{8+d}$ (Ref. 39) compounds. Here, we have modeled the hole ($h^{\cdot}$) as Pb^{3+} or O^- species, whereas electron (e') as Pb^+ or W^{5+} species.

When calculating electronic defect energy, only the large contribution due to the change in the Coloumbic interaction was taken into account. That is, the short-range interactions of O^- ion on O^{2-} lattice and Pb^{3+} ion on Pb^{2+} lattice that represent the species were taken to be the same as for the O^{2-} and Pb^{2+} ion, respectively; and the short-range interactions of W^{6+} ion was used for the electron species W^{5+}. Further, intraionic energy terms, such as the electron affinity of the O^{2-} ion [$EA_1 = 1.47$ eV, $EA_2 = -8.75$ eV (Ref. 36)] and the ionization potential terms of Pb [$IP_2 = 15.03$ eV, $IP_3 = 31.94$ eV (Ref. 40)] must be incorporated. For example, the overall energy change of reaction (3.7) is calculated by:

$$\Delta E = \tfrac{1}{2}D_e - EA_1 - EA_2 + 2IP_3 + 2E(Pb^{3+}) - E(V_{\text{O}}^{\cdot\cdot}), \tag{3.10}$$

where $D_e = 5.16$ eV is the oxygen molecule dissociation energy, $E(\text{Pb}^{3+})$ is the defect energy of substituting a Pb^{3+} ion for a regular Pb^{2+} ion, and $E(V_{\text{O}}'')$ is the vacancy energy of an oxygen ion. It should be noted that due to the uncertainties of the free-ion terms employed, e.g., the 6th ionization potential of the W atom is absent, we must be cautious in giving detailed interpretations.

The resulting energies of electronic defects, as well as the redox reactions are listed in Table V. Examination of these results shows that (i) Pb^{3+} is a favorable creation during oxidation process, the energy difference between calculated Pb^{3+} and O^- states agrees well with the reported value.[34] (ii) The oxidation reaction is most likely to occur via filling oxygen vacancies, whereas oxidation via the incorporation of interstitial oxygen seems unlikely. (iii) A comparison of the energies of oxidation and reduction indicates that the former process is more favorable. However, the high value of energy suggests that electronic defects can only predominate at high temperature, in accord with the results of observed conductivity.[29]

If the law of mass action was applied to reaction (3.7) and (3.9), we can obtain the following relations, respectively:

$$\left(\frac{\partial \ln[h]}{\partial \ln P_{\text{O}_2}}\right)_{a_{\text{PWO}}} = +\frac{1}{4}, \tag{3.11}$$

TABLE V. Oxygen migration activation energies in $PbWO_4$.

Jump path	ΔE (eV)	Jump path	ΔE (eV)
$V1$	1.94	$V2$	1.94
$V3$	0.48	$V4$	0.48
$V5$	0.48	$V6$	0.48

TABLE VI. Energies of electronic defects and redox reactions of $PbWO_4$.

(a) Electronic defect energies			
Hole states	Energy (eV)	Electron states	Energy (eV)
$Pb^{3+}(h')$	7.08	$Pb^{+}(e')$	1.84
$O^{-}(h^{\cdot})$	8.41	$W^{5+}(e')$	-
(b) Reaction energies			
Oxidation	Energy (eV)	Reduction	Energy (eV)
Eq. (3.7)	5.30	Eq. (3.9)	12.54
Eq. (3.8)	14.56		

$$\left(\frac{\partial \ln[e]}{\partial \ln P_{O_2}}\right)_{a_{PWO}} = -\frac{1}{4}, \tag{3.12}$$

in deriving that the $[V_O^{\cdot\cdot}]$ was taken as a constant, since it dominates the defects at both low [through Eq. (3.3)] and high temperature [through Eq. (3.2) or Eq. (3.9)] in PWO. Consequently, it is suggested that at low-oxygen pressures, the electronic conduction of PWO will be *n* type, whereas at high-oxygen pressures the electronic conduction will be *p* type. In general, these conclusions are consistent with experimental results.[28]

Note that from the calculated hole and electron energies we can also estimate the band gap of PWO. Compared to the experimental value of about 4.8 eV,[41] our calculated value for band gap of 8.92 eV is far higher. This overestimate is due in part to the inadequacy in the treatments of hole and electron states. For example, taking W^{5+} as an electron might give more accurate values. Also, even if the strongly localized models were valid, the omission of ligand field-splitting terms would cause appreciable errors. The error may also be partially attributed to uncertainties in the free-ion terms employed. In fact, a similar overestimate has also taken place in $KTaO_3$.[37]

IV. CONCLUSION

The present computer simulation study investigates the scheelite-type structure materials. An interatomic potential model has been constructed by transferring from the related compounds and empirically fit to the known structure properties of PWO. Valuable results, including the intrinsic defects and their clusters, transport properties, as well as the redox behavior, have been obtained. The following conclusions have emerged from our discussions.

(1) The calculation demonstrates that PbO nonstoichiometry is most possible to occur, while the oxygen Frenkel defects will only be significant at higher temperature.

(2) Through the binding energy calculations, we found, besides the formation of vacancy pairs, clusters consisting of two lead vacancies with respect to one central oxygen vacancy were possible, while cluster containing two oxygen vacancies with respect to one central lead vacancies were unstable.

(3) An analysis of activation energy reveals that oxygen vacancy migration was responsible for ionic conduction in $PbWO_4$. The calculated migration energy was 0.48 eV and in accord with the reported value. Moreover, isotropic conduction was suggested despite the tetragonal symmetry of the crystal.

(4) The study of electronic states show Pb^{3+} is a favorable result in an oxidation process. Also, the oxidation reaction is found most likely to occur via filling oxygen vacancies.

(5) Based on the redox reactions, the *n*-type conductivity at low-oxygen pressures and *p* type at high oxygen pressures are suggested.

ACKNOWLEDGMENTS

We are grateful to Dr. J. D. Gale for the GULP program and stimulating discussions. This work was financially supported by the National Science Foundation of China (Grant No. 59732040) and Science & Technology Commission of Shanghai Municipality.

*Author to whom correspondence should be addressed. Email address: xqfeng@sunm.shcnc.ac.cn

[1] F. S. Galasso, *Structure and Properties of Inorganic Solids, International Series of Monographs in Solid State Physics* (Pergamon, Oxford, 1970), Vol. 7.

[2] T. Esaks, M. Kamata, and H. Saito, Solid State Ionics **86–88**, 73 (1996).

[3] S. Takai, K. Sugiura, and T. Esaka, Mater. Res. Bull. **34**, 193 (1999).

[4] V. G. Barishevski, M. V. Korzhik, V. I. Moroz, V. B. Pavlenko, A. F. Lobko, A. A. Fedorov, V. A. Kachanov, S. G. Solovyanov, D. N. Zadneprovskii, V. A. Nefedov, P. V. Dorogovin, and L. L. Nagornaya, Nucl. Instrum. Methods Phys. Res. A **322**, 231 (1992).

[5] P. Lecoq, Nucl. Instrum. Methods Phys. Res. A **365**, 291 (1995).

[6] R. Y. Zhu, D. A. Ma, H. B. Newman, C. L. Woody, J. A. Kierstead, S. P. Stoll, and P. W. Levy, Nucl. Instrum. Methods Phys. Res. A **376**, 319 (1996).

[7] F. Nessi-Tedaldi, Nucl. Instrum. Methods Phys. Res. A **408**, 266 (1998).

[8] The Compact Muo Solenoid Experiment CMS Note, 1999/062, Nov. 23 (1999).

[9] B. Han, X. Feng, G. Hu, Y. Zhang, and Z. Yin, J. Appl. Phys. **86**, 3571 (1999).

[10] S. Baccaro, IEEE Trans. Nucl. Sci. **46**, 292 (1999).

[11] M. Martini, F. Meinardi, G. Spinolo, A. Vedda, and M. Nikl, Y. Usuki, Phys. Rev. B **60**, 4653 (1999).

[12] S. Baccaro, Phys. Status Solidi A **179**, 445 (2000).

[13] M. Nikl, K. Nitsch, J. Hybler, J. Chval, and P. Reiche, Phys. Status Solidi B **196**, K7 (1996).

[14] M. Nikl, J. Rosa, K. Nitsch, H. R. Asatryan, S. Baccaro, A. Cecilia, M. Montecchi, B. Borgia, I. Dafinei, M. Diemoz, and P. Lecoq, Mater. Sci. Forum **239–241**, 271 (1997).

[15] A. Annenkov, E. Auffray, M. V. Korzhik, P. Lecoq, and J.-P. Peigneux, Phys. Status Solidi A **170**, 47 (1998).

[16] N. F. Mott and M. J. Littlelton, Trans. Faraday Soc. **34**, 485 (1938).

[17] J. D. Gale, *General Utility Lattice Program* (Imperial College, London, 1996).

[18] J. D. Gale, Philos. Mag. B **73**, 3 (1996).

[19] C. R. A. Catlow, J. Chem. Soc., Faraday Trans. 2, **85**, 335 (1989).

[20] A. B. Liduard, J. Chem. Soc., Faraday Trans. 2, **85**, 341 (1989).

[21] M. Born, *Atomtheorie des Festen Zustandes* (Teubner, Leipzig, 1923).

[22] B. J. Dick and A. W. Overhauser, Phys. Rev. **112**, 90 (1958).

[23] J. M. Moreau, Ph. Galez, J. P. Peigneux, and M. V. Korzhik, J. Alloys Compd. **46**, 238 (1996).

[24] M. S. Islam, S. Lazure, R. Vannier, G. Nowogrocki, and G. Mairesse, J. Mater. Chem. **8**, 655 (1998).

[25] Q. Lin and X. Feng (unpublished).

[26] G. V. Lewis and C. R. A. Catlow, J. Phys. C **18**, 1149 (1985).
[27] Y. Usuki, KEK Reports No. 97-194, 1997 (unpublished).
[28] W. Van Loo, J. Solid State Chem. **14**, 359 (1975).
[29] J. A. Groenink, H. Binsma, J. Solid State Chem. **29**, 227 (1979).
[30] M. Kobayashi, Y. Usuki, M. Ishii, N. Senguttuvan, K. Tanji, M. Chiba, K. Hara, H. Takano, M. Nikl, P. Bohacek, S. Baccaro, A. Cecilia, and M. Diemoz, Nucl. Instrum. Methods Phys. Res. A **434**, 412 (1999).
[31] Q. Lin, X. Feng, Z. Man, Z. Shi, and Q. Zhang, Phys. Status Solidi A **181**, R1 (2000).
[32] M. A. Rigdon and R. E. Grace, J. Am. Ceram. Soc. **56**, 475 (1973).
[33] A. J. Edwards and L. H. Bullis, Metall. Trans. **2**, 348 (1971).
[34] Y. Zhang, N. A. W. Holzwarth, and R. T. Williams, Phys. Rev. B **57**, 12 738 (1998).
[35] C. R. A. Catlow, S. M. Tomlinson, M. S. Islam, and M. Leslie, J. Phys. C **21**, L1085 (1988).
[36] M. S. Islam, M. Leslie, S. M. Tomlinson, and C. R. A. Catlow, J. Phys. C **21**, L109 (1988).
[37] M. Exner, H. Donnerberg, C. R. A. Catlow, and O. F. Schirmer, Phys. Rev. B **52**, 3930 (1995).
[38] C. A. J. Fisher, M. S. Islam, and R. J. Brook, J. Solid State Chem. **128**, 137 (1997).
[39] M. S. Islam and L. J. Winch, Phys. Rev. B **52**, 10 510 (1995).
[40] R. J. Meyer, *Gmelin Handbook of Inorganic Chemistry*, 8th ed. (Springer-Verlag, Berlin 1987).
[41] V. Mürk, M. Nikl, E. Mihokova, and K. Nitsch, J. Phys.: Condens. Matter **9**, 249 (1997).